A *novel* humanized mouse model to study human antigen-specific cutaneous T cell responses *in vivo*.

Short title: *Skin-humanized mouse model*

Maria M. Klicznik[1], Ariane Benedetti[1], Laura M. Gail[1], Raimund Holly[1], Martin Laimer[2], Angelika Stoecklinger[1], Andreas Sir[3], Roland Reitsamer[3], Michael D. Rosenblum[4], Eva M. Murauer[5], Iris K. Gratz[1,5,6]

[1] Department of Biosciences, University of Salzburg, Salzburg, Austria

[2] Department of Dermatology, University Hospital of the Paracelsus Medical University Salzburg, Austria

[3]Breast Center University Hospital of the Paracelsus Medical University Salzburg, Austria

[4]Department of Dermatology, University of California, San Francisco CA 94143, USA.

[5]Division of Molecular Dermatology and EB House Austria, Department of Dermatology, Paracelsus Medical University Salzburg, Austria

[6]Benaroya Research Institute, 1201 9th AVE, Seattle, WA 98101 USA

Abstract

Human skin contains a significant number of T cells that support tissue homeostasis and provide protective immunity. T cell function in human skin is difficult to study due to a lack of adequate *in vivo* models. In this study we used immunodeficient NOD-*scid IL2rγ*^{null} (NSG) mice that carried *in vivo*-generated engineered skin (ES) and received adoptively transferred human peripheral blood mononuclear cells. ES were generated from keratinocytes and fibroblasts only and initially contained no skin-resident immune cells. This reductionist system allowed us to study T cell recruitment and function in non-inflamed and non-infected human skin. We found that functional human T cells specifically infiltrated the human skin tissue and responded to microbial antigen *in vivo*. Importantly, T cell maintenance and function was supported by the microenvironment of human skin. We have thus generated a novel mouse model with broad

utility in studies of human cutaneous antigen-specific T cell responses and the role of the skin microenvironment to skin immunity *in vivo*.

Introduction

As the body's outermost barrier, the skin represents a unique and complex immunological organ. As such, healthy human skin contains around twice the number of T cells found in the blood of which the majority are memory T cells (Bos et al. 1989; Clark et al. 2006) that support tissue homeostasis and ensure adequate response to pathogens (Di Meglio et al. 2011; Klicznik et al. 2018; Nestle et al. 2009). Although significant advances in understanding the role of the skin microenvironment on T cell function and memory development in murine skin have been made (Mackay et al. 2015; Mackay et al. 2013; Pan et al. 2017), the specific contribution of keratinocyte- and fibroblast-derived signals to cutaneous immunity in human skin remain poorly understood. T cell responses are strongly influenced by the surrounding tissue (Hu and Pasare 2013; McCully et al. 2012), and T cells at different barrier sites show distinct functional and metabolic properties (Kumar et al. 2017; Pan et al. 2017), therefore it is crucial to study cutaneous immunity within its physiological compartment *in vivo*. Due to fundamental structural differences between human and murine skin, as well as a lack of direct correspondence between human and murine immune cell populations (Di Meglio et al. 2011; Gudjonsson et al. 2007; Perlman 2016; Shay et al. 2013), direct translation from the murine cutaneous immune system can be difficult. This emphasizes the need for mouse models that faithfully replicate conditions found in human skin. Humanized mice, in which immunodeficient mice are adoptively transferred with human peripheral blood mononuclear cells (PBMC) and transplanted with human full thickness skin derived from either healthy donors or patients with skin diseases are currently used to study human skin immunology *in vivo* (Boyman et al. 2004; King et al. 2009; Watanabe et al. 2015). In these models the rejection of skin allografts and xenogenic graft versus host disease (GvHD) development can

be readily studied (Racki et al. 2010), but antigen-specific activation of T cells has been much harder to follow. Additionally, if obtained from adult donors full-thickness skin grafts contain resident immune cells (Clark et al. 2006; Racki et al. 2010; Sanchez Rodriguez et al. 2014; Watanabe et al. 2015), making it difficult to functionally analyze and manipulate discrete skin-tropic T cell populations.

We hypothesized that humanized mice reconstituted with simplified human skin consisting only of keratinocytes and fibroblasts would provide a reductionist system allowing us to study human T cell recruitment and function in human skin in absence of acute inflammation. To this end, we used NOD-*scid IL2rγ*^{null} (NSG) mice that were adoptively transferred with human PBMC and carried *in vivo*-generated engineered skin (ES). This model serves as a novel platform for studying human cutaneous antigen-specific T cell responses, and the contribution of the skin microenvironment to skin immunity *in vivo*. Additionally, we provide a method to stimulate robust antigen-specific memory responses of cutaneous T cells in this system.

Results

Human T cells specifically infiltrate human engineered skin in a xenograft mouse model.

To follow human skin infiltration by autologous human immune cells, we generated engineered skin (ES) from human keratinocytes and fibroblasts isolated from healthy human skin and immortalized (Merkley et al. 2009). ES was generated as described before (Wang et al. 2000) and allowed to heal and differentiate for a minimum of 30 days (Fig.1a). H&E staining revealed that the ES displayed histological features of human and not murine skin. Additionally, organotypic proteins such as human type VII collagen at the basement membrane of the ES and human cytokeratin 5/6 within the correct epidermal layers of the ES confirmed correct differentiation and human origin (Fig.1b). In parallel, human PBMC from the skin donor were isolated and stored in liquid nitrogen until use (Fig.1a). After complete

wound healing of the ES PBMC were adoptively transferred, thus creating a mouse model designated huPBMC-ES-NSG.

Engraftment of human $CD45^+$ cells was detectable after 14 days in the spleen and after 21 days in the ES (Fig. 1c-d). After a period of 18 - 34 days mean levels of human $CD45^+$ cells in spleen and ES were at >18% (Fig. 1e). The majority of human cells (>94%) in spleen and ES were $CD3^+$ T cells (Fig. 1f) and human $CD3^+$ cells preferentially infiltrated human ES not the adjacent murine skin (Fig. 1g). $CD4^+$ and $CD8^+$ as well as $TCR\gamma\delta^+$ T cells engrafted within the spleen and ES at levels comparable to human PBMC and skin (Fig. 1h-i). The ratios of $CD4^+$ and $CD8^+$ T cells engrafting in spleen and ES reflected the physiological levels found in human PBMC and skin, respectively (Table in Fig. 1j).

In previous studies development of xenogeneic graft versus host disease (xeno-GvHD) occurred around 5 weeks after adoptive transfer of 10^7 human PBMC into NSG mice (Ali et al. 2012; King et al. 2008). To delay the development of GvHD we reduced cell numbers to 1.8 - $3x10^6$ /mouse. Additionally, we limited all experiments to 35 days, which was before onset of GvHD thus avoiding convoluting effects on our studies.

Taken together, these data illustrate that the human T cell compartment can be reconstituted in spleen and ES of the huPBMC-ES-NSG mouse. Next, we sought to determine whether the model was suitable to study human T cell function within human skin *in vivo*.

Cutaneous and splenic T cells from huPBMC-ES-NSG maintain the functional profile of T cells found in human skin and blood

We assessed the function of splenic and skin T cells following *ex vivo* stimulation and intracellular cytokine staining. Production of the Th2, Th17 and Th22 cytokines IL-13, IL-17 and IL-22, respectively, were preserved in $CD4^+$ T cells isolated from the huPBMC-ES-NSG mouse when compared to T cells from human blood and skin(Fig. 2a-b; e-g). By contrast,

increased percentages of $CD4^+$ T cells isolated from the spleen and ES produced GM-CSF (Fig. 2c; h-i). Interestingly while $IFN\gamma^+CD4^+$ cells were increased in the spleen when compared to PBMC, the proportion of IFNγ producing $CD4^+$ cells within the ES was comparable to skin from healthy donors (Fig. 2i). In addition to conventional T cells, $CD4^+CD25^+Foxp3^+$ regulatory T cells engrafted within the spleen and ES (Fig. 2d; j). Analogous to the cytokine profiles of splenic and cutaneous $CD4^+$ T cells, we assessed the cytokine secretion of $CD8^+$ T cells isolated from spleen and ES (Fig. 3). The cytokine profiles of $CD8^+$ T cells in ES and spleen were comparable to healthy human skin and PBMC with the exception of GM-CSF, which was increased within the ES, similar to the $CD4^+$ T cell population.

Engrafted T cells share a skin-homing memory-like phenotype

Since $CD4^+$ T cells represent the majority of skin-homing and -resident T cells (Clark et al. 2006; Watanabe et al. 2015), we focused on the function of cutaneous $CD4^+$ T cells. Confirming previous studies of PBMC engraftment in NSG mice, we found that human $CD4^+$ T cells isolated from mice did not express markers of naïve T cells such as CCR7 and CD45RA despite being present in the ingoing PBMC population (Ali et al. 2012) (Fig. 4a). Additionally, around half of them expressed cutaneous leukocyte antigen (CLA), a glycan moiety that promotes skin-homing (Clark et al. 2006) (Fig. 4b). Taken together these data indicate that engrafted $CD4^+$ T cells show a skin-tropic, memory-like phenotype.

Cutaneous $CD4^+$ T cells are locally activated by microbial antigen

Skin $CD4^+$ T cells play a crucial role in controlling cutaneous microbes (Belkaid and Tamoutounour 2016). Their specific role in responses against the commensal fungus *Candida albicans* (Lagunes and Rello 2016) is underlined by the fact that primary and acquired immunodeficiencies that lead to the impairment of $CD4^+$ T cell immunity can cause

pathogenic *C.albicans* infections (Gosselin et al. 2010; Klein et al. 1984; Lagunes and Rello 2016; Ling et al. 2015; Puel et al. 2011). Consistent with that, the human circulating T cell pool contains *C.albicans*-specific memory T cells (Acosta-Rodriguez et al. 2007; Hernández-Santos and Gaffen 2012).

We hypothesized that memory T cells specific for *C.albicans,* engraft in the ES and can mount a local antigen-specific T cell response upon encounter of microbial antigen. Therefore, we applied heat killed *C.albicans* (HKCA) to the ES *in vivo.* Injection of free HKCA failed to elicit a detectable expansion or proliferation in the spleen or ES of treated mice (Supp. Fig.1a-b; not shown). This was likely due to poor engraftment of HLA-DR$^+$CD3$^-$ antigen presenting cells (APC) within the NSG strain (King et al. 2009) (Supp. Fig. 1c-d). Since *C.albicans* specific T cell responses depend on the presence of HLA-DR$^+$ APC (Acosta-Rodriguez et al. 2007; Park et al. 2018) we pulsed autologous monocyte derived dendritic cells (moDC) with HKCA (HKCA/moDC) and injected these intradermally into the ES. LPS activated moDC (LPS/moDC) served as a control for non-specific activation of T cells by cytokines derived from activated APCs. Injections were repeated 3 times within 7 days and were followed by flow cytometry analysis of T cells isolated from the ES and spleen one week after the last injection (Fig. 5a). Whereas the proportion of human CD45$^+$ cells in the spleen remained unaffected irrespective of the treatment, a slight increase in the percentage of human CD45$^+$ cells could be detected in ES injected with HKCA/moDC compared to LPS/moDC injected ES (Fig. 5b). Additionally, an increased proportion of CD4$^+$ T cells expressed the proliferation marker Ki67 and significantly upregulated CD25 upon injection of HKCA/moDC, indicating activation of CD4$^+$ T cells in response to the encountered antigen (Fig. 5c). Interestingly the increased proliferation and activation of CD4$^+$ T cells in response to antigen was locally restricted to the injected ES and absent in splenic T cells (Supp. Fig. 2a-b).

Together these data show that the huPBMC-ES-NSG model provides a tool to monitor antigen-specific T cell responses within human skin *in vivo*.

Antigen-specific T cell responses remain detectable in donor-mismatched skin tissue

So far, we used a completely matched system where ES, PBMC and moDC were from the same donor. However, access to skin that is matched to the PBMC, presents a limiting factor in studies of human immune responses. To broaden the model's applicability, we sought to determine whether antigen-specific T cell responses could still be detected in the skin when using donor-mismatched tissues. Therefore, we compared cutaneous $CD4^+$ T cell responses to HKCA in donor-matched and -mismatched ES. ES were generated from two different donors (donor A or B) designated ES-NSG-A and ES-NSG-B. After complete wound healing, both recipients received PBMC from donor A and were injected intradermally with matched LPS/moDC or HKCA/moDC (from donor A) (Fig. 5d).

Significantly higher proportions of $CD4^+$ T cells from ES injected with HKCA/moDC expressed HLA-DR compared to LPS/moDC injected ES, indicating recent antigen-specific activation (Holling et al. 2004; Ko 1979; Oshima and Eckels 1990) (Fig. 5e). Moreover, ES injected with HKCA/moDC contained an increased proportion of $CD4^+$ T cells secreting IL17 and TNFα compared to LPS/moDC (Fig. 5f-g). Importantly, IFNγ^+ (Fig. 5h) and HLA-DR^+ $CD4^+$ cell proportions (Fig. 5e) were not expanded in allogeneic skin compared to the autologous setting. Additionally, CD4:CD8 ratios remained unchanged between skin T cells from matched and mismatched HKCA/moDC injected ES (Fig. 5i). Splenic $CD4^+$ T cells showed high levels of activation irrespective of the injected moDC and no HKCA-specific cytokine production (Supp.Fig. 2c-f) and, splenic $CD4^+$:$CD8^+$ T cell ratios were unaltered in response to the allogeneic ES (Supp.Fig. 2g), indicating the absence of a systemic response. Together, these data suggest that T cells were not activated by allogeneic keratinocytes or

fibroblasts and that mismatched tissues still allow the study human antigen-specific cutaneous $CD4^+$ T cell responses in the huPBMC-ES-NSG model.

Human skin tissue promotes T cell maintenance and function

Based on the finding that human T cells preferentially infiltrated the human over the murine skin and T cells within the ES closely resembled T cells found in human skin (Fig. 1-3), we hypothesized, that human skin and ES provide similar signals to infiltrating T cells. Interestingly skin-derived chemokines, such as CCL2, CCL5, CXCL10 and CXCL12 (Fig. 6 a-d) and cytokines involved in T cell survival and maintenance, such as IL7 and IL15 were detectable at comparable levels in ES and normal human skin (Fig. 6 e,f). Based on these data, we hypothesized that the antigen-specific T cell response we detected was dependent on skin tissue-derived signals. To test this, we injected either the ES of huPBMC-ES-NSG or a defined area of murine skin on the back of huPBMC-NSG mice with autologous HKCA/moDC or LPS/moDC (Fig. 6g). Compared to ES treated with HKCA/moDC, significantly lower numbers of $CD3^+$ cells infiltrated the murine skin. Importantly their frequency remained unaltered upon injection of HKCA/moDC, indicating a lack of antigen-specific activation (Fig. 6h). This suggests that the *C.albicans* specific T cell response detected in the huPBMC-ES-NSG model is not only a memory re-call response that is elicited by T cell-APC interaction, but requires tissue derived signals to support full memory T cell function.

Discussion

The majority of T cells in healthy human skin are CD45RO memory T cells that ensure adequate protective immunity on this peripheral barrier site (Bos et al. 1989; Klicznik et al. 2018; Watanabe et al. 2015). Most of our understanding of the development and function of protective T cell immunity in the skin is based on research using animal models with limited

direct translation to humans (Di Meglio et al. 2011; Gudjonsson et al. 2007; Schreiner and King 2018). Therefore skin-humanized mouse models present a powerful platform to study cutaneous immune processes *in vivo*. Existing models in which PBMC and skin are grafted have been most useful for studying inflammatory processes of the skin (Boyman et al. 2004; Issa et al. 2010; Racki et al. 2010; Watanabe et al. 2015) but studies of human cutaneous immunity in steady-state *in vivo* have been difficult to realize. Additionally, healthy human skin contains a variety of adaptive and innate immune cells that impact the outcome of any intervention and study (Di Meglio et al. 2011; Klicznik et al. 2018; Pasparakis et al. 2014). Studying distinct immune processes in the skin requires simple traceable models, in which specific components can be independently manipulated. In that respect, neonatal foreskin grafts that contain 45-fold less T cells than adult human skin have been used to reduce the impact of resident cells (Watanabe et al. 2015), but even this tissue already contains T cells (Schuster et al. 2012). Here we combined engineered skin (ES) (Wang et al. 2000) devoid of any resident leukocytes, and adoptive transfer of human PBMC into immunodeficient NSG mice to generate a humanized mouse model (huPBMC-ES-NSG) that allows for specific study of individual immune cell populations, as well as the impact of tissue-derived signals on immunological processes in the skin.

Importantly, the use of ES permits precise control over the cell populations that partake in a specific immune response and targeted manipulation of keratinocytes and fibroblasts using CRISPR/Cas9 will facilitate to study the influence of selected pathways and the effects of these alterations on cutaneous immunity *in vivo*.

Poor engraftment of APC can limit antigen-specific T cell responses *in vivo* (King et al. 2009), which can be partly overcome by injection of DC loaded with antigen (Harui et al. 2011). However, we have found that antigen-specific recall responses require the support of the micromilieu, such as tissue-derived IL15 and IL7 (Belarif et al. 2018; Wang et al. 2011) and $CD4^+$ T cells failed to respond to antigen presented in murine skin. Importantly, we found

that healthy human skin- and ES-derived signals were remarkably similar, especially chemokines and cytokines involved in T cell recruitment and activation, such as CCL2 (Carr et al. 1994), CCL5 (Kawai et al. 1999), CXCL10 (Fukui et al. 2013), CXCL12 (Nanki and Lipsky 2001) and T cell function and maintenance, like IL7 (Adachi et al. 2015; Belarif et al. 2018) and IL15 (Adachi et al. 2015; Wang et al. 2011). This indicates that the huPBMC-NSG-ES model enables us to study the contribution of tissue-derived cues on cutaneous T cell maintenance and function.

Interestingly, the antigen-specific response was detectable in both, an autologous and an allogeneic setting. Thus, access to matched tissue samples is not limiting the study of cutaneous T cell responses in these humanized mice.

By engineering human skin tissue, we created an environment that allows the study of cutaneous T cell responses in absence of inflammation or infection *in vivo*. Additionally, the model may serve as a platform to test novel therapeutic interventions to treat cutaneous inflammation, tumors or autoimmune diseases. Taken together, the huPBMC-ES-NSG model provides a highly versatile tool to study cutaneous T cell responses and study and manipulate tissue-derived signals that impact skin immunity.

Material and Methods

Mice. Animal studies were approved by the Austrian Federal Ministry of Science, Research and Economy. NOD.Cg-Prkdcscid Il2rgtm1Wjl/SzJ (NSG) mice were obtained from The Jackson Laboratory and bred and maintained in a specific pathogen-free facility in accordance with the guidelines of the Central Animal Facility of the University of Salzburg.

Human specimens. Normal human skin was obtained from patients undergoing elective surgery, in which skin was discarded as a routine procedure. Blood and/or discarded healthy skin was donated upon written informed consent at the University Hospital Salzburg, Austria.

PBMC isolation for adoptive transfer into NSG recipients and flow cytometry. Human PBMC were isolated from full blood using Ficoll-Hypaque (GE-Healthcare; GE17-1440-02) gradient separation. PBMC were frozen in FBS with 10% DMSO (Sigma-Aldrich; D2650), and before adoptive transfer thawed and rested overnight at 37°C and 5% CO_2 in RPMIc (RPMI 1640 (Gibco; 31870074) with 5% human serum (Sigma-Aldrich; H5667 or H4522), 1% penicillin/streptomycin (Sigma-Aldrich; P0781), 1% L-Glutamine (Gibco; A2916801), 1% NEAA (Gibco; 11140035), 1% Sodium-Pyruvate (Sigma-Aldrich; S8636) and 0.1% β-Mercaptoethanol (Gibco; 31350-010). Cells were washed and 1.8-3x10^6 PBMC/mouse intravenously injected. Murine neutrophils were depleted with mLy6G (Gr-1) antibody (BioXcell; BE0075) intraperitoneally every 5-7 days as described before (Racki et al. 2010).

Generation of engineered skin (ES). Human keratinocytes and fibroblasts were isolated from human skin and immortalized using human papilloma viral oncogenes E6/E7 HPV as previously described (Merkley et al. 2009). Cells were cultured in Epilife (Gibco, MEPICF500) or DMEM (Gibco; 11960-044) containing 2% L-Glutamine, 1% Pen/Strep, 10% FBS, respectively. Per mouse, 1-2x10^6 keratinocytes were mixed 1:1 with autologous fibroblasts in 400µl MEM (Gibco; 11380037) containing 1% FBS, 1% L-Glutamine and 1% NEAA for *in vivo* generation of engineered skin as described (Wang et al. 2000).

T cell isolation from skin tissues for flow cytometry. Healthy human skin and ES were digested as previously described (Sanchez Rodriguez et al. 2014). Approximately 1cm^2 of skin was digested overnight in 5%CO_2 at 37°C with 3ml of digestion mix containing 0.8mg/ml Collagenase Type 4 (Worthington; #LS004186) and 0.02mg/ml DNase (Sigma-Aldrich; DN25) in RPMIc. ES were digested in 1ml of digestion mix. Samples were filtered, washed and stained for flow cytometry or stimulated for intracellular cytokine staining. Approx. 3 cm^2 of shaved dorsal mouse skin were harvested and single cell suspensions prepared as described (Gratz et al. 2014) and stained for flow cytometry.

Flow cytometry. Cells were stained in PBS for surface markers. For detection of intracellular cytokine production, spleen and skin single cell suspensions and PBMC were stimulated with 50 ng/ml PMA (Sigma-Aldrich; P8139) and 1 µg/ml Ionomycin (Sigma-Aldrich; I06434) with 10 µg/ml Brefeldin A (Sigma-Aldrich; B6542) for 3.5 hrs. For permeabilization and fixation Cytofix/Cytoperm (BectonDickinson; RUO 554714) or Foxp3 staining kit (Invitrogen; 00-5523-00) were used. Data were acquired on LSR Fortessa (BD Biosciences) or Cytoflex LS (Beckman.Coulter) flow cytometers and analyzed using FlowJo software (Tree Star, Inc.) A detailed list of the used antibodies can be found in the Supplements.

Histological staining of skin sections. Normal human skin, ES and adjacent murine skin were frozen in TissueTek (Sakura; TTEK). 7 µm cryosections were stained with Hemalum solution acid (Carl Rorth; T865.1) and Eosin Y aqueous solution (Sigma, 201192A). Human type VII collagen was stained by immunofluorescence using anti-human type VII collagen antibody and goat anti-rabbit A488 as secondary antibody,

ProLong™ Gold Antifade Mountant with DAPI, (Invitrogen; P36931) was used for nuclear staining and mounting. For immunohistochemistry paraffin-embedded normal human skin and ES was stained for human Cytokeratin 5/6 according to the manufacturer's protocol using a Ventana BenchMark Series automated slide stainer with ultraView Universal DAB Detection kit (Roche, 760-500).

Generation of monocyte derived dendritic cells (moDC)

moDC were generated from frozen PBMC similar to what has been described previously (Sallusto and Lanzavecchia 1994). Briefly, PBMC were thawed and monocytes adhered for 75 min at 37 °C and 5% CO_2 in DC medium (RPMI 1640: 10% FBS, 2 mM L-Glutamine, 100 U/ml penicillin/streptomycin, 50 µM β-mercaptoethanol). After washing, adherent monocytes were cultured in DC medium supplemented with 50 ng/ml GM-CSF (ImmunoTools; 11343127) and 50 ng/ml IL-4 (ImmunoTools; 11340047) for 7 days to generate immature DC. After 6 days, cells were harvested and re-plated in DC medium without cytokines. For activation, moDCs were cultured for 9-13 hrs with 5ng/ml LPS (Sigma-Aldrich; L2880**)** or 10^6 cells/ml heat killed *Candida albicans* (eubio; tlrl-hkca). 1.8-3x10^4 moDC/mouse were intradermally injected in 50µl PBS/mouse.

ProcartaPlex™ immunoassays from human skin and engineered skin

Human skin or ES from huPBMC-ES-NSG mice were stored at -70°C until use. Skin was taken up in PBS with Protease Inhibitor Cocktail (1:100) (Sigma-Aldrich; P8340) at 1ml/50mg skin, homogenized and filtered through 0.22µm SpinX columns. Suspensions were stored at -70°C until use. ProcartaPlex immunoassay was performed according to the manufacturer's protocol and measured using Luminex Magpix® system.

Statistical analysis. Statistical significance was calculated with Prism 7.0 software (GraphPad) by one-way ANOVA with Tukey's multiple comparisons test, or by un-paired student's t-test as indicated. Error bars indicate mean +/- standard deviation.

Conflict of Interest.

The authors declare no conflict of interest.

Acknowledgements.

We especially thank all human subjects for blood and skin donation and the nurses at the Breast Center University Hospital of the Paracelsus Medical University Salzburg, Austria. We thank Dr. Stefan Hainzl, EB House Austria, Department of Dermatology, University Hospital of the Paracelsus Medical University Salzburg, Austria, for the immortalization of primary human keratinocytes and fibroblasts. We thank Monika Prinz from the Department of Dermatology at the University Hospital of the Paracelsus Medical University Salzburg, Austria for help with the IHC staining and Peter Steinbacher from the Department of Biosciences at the University of Salzburg, Austria, for support with microscopy. This work was supported by the Focus Program "ACBN" of the University of Salzburg, Austria, by a grant from the Dystrophic Epidermolysis Bullosa Research Association (DEBRA) International and DEBRA Austria, and NIH grant R01AI127726. MMK is part of the PhD program Immunity in Cancer and Allergy, funded by the Austrian Science Fund (FWF, grant W 1213) and was recipient of a DOC Fellowship of the Austrian Academy of Sciences.

Author Contributions.

IGK, EMM, MDR and MMK conceptualized the study, MMK, EMM and IGK designed the experiments; MMK, AB, LMG and RH acquired the data; ML performed IHC staining, AS, RR, and A.Sir acquired human samples; MMK performed data analysis, MMK and IGK

interpreted the data and wrote the manuscript. All authors reviewed the final version of the manuscript. IKG and EMM supervised the project.

References

Acosta-Rodriguez EV, Rivino L, Geginat J, Jarrossay D, Gattorno M, Lanzavecchia A, et al. Surface phenotype and antigenic specificity of human interleukin 17-producing T helper memory cells. Nat. Immunol. 2007;8(6):639–46

Adachi T, Kobayashi T, Sugihara E, Yamada T, Ikuta K, Pittaluga S, et al. Hair follicle-derived IL-7 and IL-15 mediate skin-resident memory T cell homeostasis and lymphoma. Nat. Med. 2015;21(11):1272–9

Ali N, Flutter B, Sanchez Rodriguez R, Sharif-Paghaleh E, Barber LD, Lombardi G, et al. Xenogeneic Graft-versus-Host-Disease in NOD-scid IL-2Rγnull Mice Display a T-Effector Memory Phenotype. PLoS ONE. 2012;7(8) Available from: https://www.ncbi.nlm.nih.gov/pmc/articles/PMC3429415/

Belarif L, Mary C, Jacquemont L, Mai HL, Danger R, Hervouet J, et al. IL-7 receptor blockade blunts antigen-specific memory T cell responses and chronic inflammation in primates. Nat. Commun. 2018;9 Available from: https://www.ncbi.nlm.nih.gov/pmc/articles/PMC6203796/

Belkaid Y, Tamoutounour S. The influence of skin microorganisms on cutaneous immunity. Nat. Rev. Immunol. 2016;16(6):353–66

Bos JD, Hagenaars C, Das PK, Krieg SR, Voorn WJ, Kapsenberg ML. Predominance of "memory" T cells (CD4+, CDw29+) over "naive" T cells (CD4+, CD45R+) in both normal and diseased human skin. Arch. Dermatol. Res. 1989;281(1):24–30

Boyman O, Hefti HP, Conrad C, Nickoloff BJ, Suter M, Nestle FO. Spontaneous Development of Psoriasis in a New Animal Model Shows an Essential Role for Resident T Cells and Tumor Necrosis Factor-α. J. Exp. Med. 2004;199(5):731–6

Carr MW, Roth SJ, Luther E, Rose SS, Springer TA. Monocyte chemoattractant protein 1 acts as a T-lymphocyte chemoattractant. Proc. Natl. Acad. Sci. U. S. A. 1994;91(9):3652–6

Clark RA, Chong B, Mirchandani N, Brinster NK, Yamanaka K-I, Dowgiert RK, et al. The vast majority of CLA+ T cells are resident in normal skin. J. Immunol. Baltim. Md 1950. 2006;176(7):4431–9

Di Meglio P, Perera GK, Nestle FO. The multitasking organ: recent insights into skin immune function. Immunity. 2011;35(6):857–69

Fukui A, Ohta K, Nishi H, Shigeishi H, Tobiume K, Takechi M, et al. Interleukin-8 and CXCL10 expression in oral keratinocytes and fibroblasts via Toll-like receptors. Microbiol. Immunol. 2013;57(3):198–206

Gosselin A, Monteiro P, Chomont N, Diaz-Griffero F, Said EA, Fonseca S, et al. Peripheral blood CCR4+CCR6+ and CXCR3+CCR6+CD4+ T cells are highly permissive to HIV-1 infection. J. Immunol. Baltim. Md 1950. 2010;184(3):1604–16

Gratz IK, Rosenblum MD, Maurano MM, Paw JS, Truong H-A, Marshak-Rothstein A, et al. Cutting edge: Self-antigen controls the balance between effector and regulatory T cells in peripheral tissues. J. Immunol. Baltim. Md 1950. 2014;192(4):1351–5

Gudjonsson JE, Johnston A, Dyson M, Valdimarsson H, Elder JT. Mouse models of psoriasis. J. Invest. Dermatol. 2007;127(6):1292–308

Harui A, Kiertscher SM, Roth MD. Reconstitution of huPBL-NSG Mice with Donor-Matched Dendritic Cells Enables Antigen-Specific T-cell Activation. J. Neuroimmune Pharmacol. 2011;6(1):148–57

Hernández-Santos N, Gaffen SL. Th17 cells in immunity to Candida albicans. Cell Host Microbe. 2012;11(5):425–35

Holling TM, Schooten E, van Den Elsen PJ. Function and regulation of MHC class II molecules in T-lymphocytes: of mice and men. Hum. Immunol. 2004;65(4):282–90

Hu W, Pasare C. Location, location, location: tissue-specific regulation of immune responses. J. Leukoc. Biol. 2013;94(3):409–21

Issa F, Hester J, Goto R, Nadig SN, Goodacre TE, Wood K. Ex vivo-expanded human regulatory T cells prevent the rejection of skin allografts in a humanized mouse model. Transplantation. 2010;90(12):1321–7

Kawai T, Seki M, Hiromatsu K, Eastcott JW, Watts GF, Sugai M, et al. Selective diapedesis of Th1 cells induced by endothelial cell RANTES. J. Immunol. Baltim. Md 1950. 1999;163(6):3269–78

King MA, Covassin L, Brehm MA, Racki W, Pearson T, Leif J, et al. Human peripheral blood leucocyte non-obese diabetic-severe combined immunodeficiency interleukin-2 receptor gamma chain gene mouse model of xenogeneic graft-versus-host-like disease and the role of host major histocompatibility complex. Clin. Exp. Immunol. 2009;157(1):104–18

King M, Pearson T, Shultz LD, Leif J, Bottino R, Trucco M, et al. A new Hu-PBL model for the study of human islet alloreactivity based on NOD-scid mice bearing a targeted mutation in the IL-2 receptor gamma chain gene. Clin. Immunol. Orlando Fla. 2008;126(3):303–14

Klein RS, Harris CA, Small CB, Moll B, Lesser M, Friedland GH. Oral candidiasis in high-risk patients as the initial manifestation of the acquired immunodeficiency syndrome. N. Engl. J. Med. 1984;311(6):354–8

Klicznik MM, Szenes-Nagy AB, Campbell DJ, Gratz IK. Taking the lead - how keratinocytes orchestrate skin T cell immunity. Immunol. Lett. 2018;200:43–51

Ko HS. Ia determinants on stimulated human T lymphocytes. Occurrence on mitogen- and antigen-activated T cells. J. Exp. Med. 1979;150(2):246–55

Kumar BV, Ma W, Miron M, Granot T, Guyer RS, Carpenter DJ, et al. Human Tissue-Resident Memory T Cells Are Defined by Core Transcriptional and Functional Signatures in Lymphoid and Mucosal Sites. Cell Rep. 2017;20(12):2921–34

Lagunes L, Rello J. Invasive candidiasis: from mycobiome to infection, therapy, and prevention. Eur. J. Clin. Microbiol. Infect. Dis. Off. Publ. Eur. Soc. Clin. Microbiol. 2016;35(8):1221–6

Ling Y, Cypowyj S, Aytekin C, Galicchio M, Camcioglu Y, Nepesov S, et al. Inherited IL-17RC deficiency in patients with chronic mucocutaneous candidiasis. J. Exp. Med. 2015;212(5):619–31

Mackay LK, Rahimpour A, Ma JZ, Collins N, Stock AT, Hafon M-L, et al. The developmental pathway for CD103(+)CD8+ tissue-resident memory T cells of skin. Nat. Immunol. 2013;14(12):1294–301

Mackay LK, Wynne-Jones E, Freestone D, Pellicci DG, Mielke LA, Newman DM, et al. T-box Transcription Factors Combine with the Cytokines TGF-β and IL-15 to Control Tissue-Resident Memory T Cell Fate. Immunity. 2015;43(6):1101–11

McCully ML, Ladell K, Hakobyan S, Mansel RE, Price DA, Moser B. Epidermis instructs skin homing receptor expression in human T cells. Blood. 2012;120(23):4591–8

Merkley MA, Hildebrandt E, Podolsky RH, Arnouk H, Ferris DG, Dynan WS, et al. Large-scale analysis of protein expression changes in human keratinocytes immortalized by human papilloma virus type 16 E6 and E7 oncogenes. Proteome Sci. 2009;7:29

Nanki T, Lipsky PE. Stimulation of T-Cell Activation by CXCL12/Stromal Cell Derived Factor-1 Involves a G-Protein Mediated Signaling Pathway. Cell. Immunol. 2001;214(2):145–54

Nestle FO, Di Meglio P, Qin J-Z, Nickoloff BJ. Skin immune sentinels in health and disease. Nat. Rev. Immunol. 2009;9(10):679–91

Oshima S, Eckels DD. Selective signal transduction through the CD3 or CD2 complex is required for class II MHC expression by human T cells. J. Immunol. Baltim. Md 1950. 1990;145(12):4018–25

Pan Y, Tian T, Park CO, Lofftus SY, Mei S, Liu X, et al. Survival of tissue-resident memory T cells requires exogenous lipid uptake and metabolism. Nature. 2017;543(7644):252–6

Park CO, Fu X, Jiang X, Pan Y, Teague JE, Collins N, et al. Staged development of long-lived T-cell receptor αβ TH17 resident memory T-cell population to Candida albicans after skin infection. J. Allergy Clin. Immunol. 2018;142(2):647–62

Pasparakis M, Haase I, Nestle FO. Mechanisms regulating skin immunity and inflammation. Nat. Rev. Immunol. 2014;14(5):289–301

Perlman RL. Mouse models of human disease. Evol. Med. Public Health. 2016;2016(1):170–6

Puel A, Cypowyj S, Bustamante J, Wright JF, Liu L, Lim HK, et al. Chronic mucocutaneous candidiasis in humans with inborn errors of interleukin-17 immunity. Science. 2011;332(6025):65–8

Racki WJ, Covassin L, Brehm M, Pino S, Ignotz R, Dunn R, et al. NOD-scid IL2rgamma(null) mouse model of human skin transplantation and allograft rejection. Transplantation. 2010;89(5):527–36

Sallusto F, Lanzavecchia A. Efficient presentation of soluble antigen by cultured human dendritic cells is maintained by granulocyte/macrophage colony-stimulating factor plus interleukin 4 and downregulated by tumor necrosis factor alpha. J. Exp. Med. 1994;179(4):1109–18

Sanchez Rodriguez R, Pauli ML, Neuhaus IM, Yu SS, Arron ST, Harris HW, et al. Memory regulatory T cells reside in human skin. J. Clin. Invest. 2014;124(3):1027–36

Schreiner D, King CG. CD4+ Memory T Cells at Home in the Tissue: Mechanisms for Health and Disease. Front. Immunol. 2018;9 Available from: https://www.frontiersin.org/articles/10.3389/fimmu.2018.02394/full

Schuster C, Vaculik C, Prior M, Fiala C, Mildner M, Eppel W, et al. Phenotypic characterization of leukocytes in prenatal human dermis. J. Invest. Dermatol. 2012;132(11):2581–92

Shay T, Jojic V, Zuk O, Rothamel K, Puyraimond-Zemmour D, Feng T, et al. Conservation and divergence in the transcriptional programs of the human and mouse immune systems. Proc. Natl. Acad. Sci. 2013;110(8):2946–51

Wang X, Berger C, Wong CW, Forman SJ, Riddell SR, Jensen MC. Engraftment of human central memory-derived effector CD8+ T cells in immunodeficient mice. Blood. 2011;117(6):1888–98

Wang CK, Nelson CF, Brinkman AM, Miller AC, Hoeffler WK. Spontaneous cell sorting of fibroblasts and keratinocytes creates an organotypic human skin equivalent. J. Invest. Dermatol. 2000;114(4):674–80

Watanabe R, Gehad A, Yang C, Campbell L, Teague JE, Schlapbach C, et al. Human skin is protected by four functionally and phenotypically discrete populations of resident and recirculating memory T cells. Sci. Transl. Med. 2015;7(279):279ra39

Figure Legends

Figure 1: Engineered skin resembles human skin and is preferentially infiltrated by human T cells upon adoptive PBMC transfer. (**a**) Schematic of the huPBMC-ES-NSG model. (**b**) H&E staining and immunofluorescence staining of human type VII collagen in human skin, ES and murine skin, as indicated (upper two panels) as well as immunohistochemical staining of human Cytokeratin 5/6 in human skin and ES (lower panel). White bar = 100µm (**c-g**) Single cell suspensions of spleen and ES of huPBMC-ES-NSG mice were analyzed by flow cytometry. Each data point represents an individual human donor or experimental mouse. Circles represent data collected from huPBMC-ES-NSG mice using tissue of donor WT85 and squares donor WT70. The different fillings of the symbols indicate independent experiments. (**c**) Representative flow cytometry analysis and (**d**) graphical summary of proportion of human $CD45^+$ cell as % of live cells in the lymphocyte gate in spleen and ES at indicated time points after adoptive transfer of $2.5x10^6$ PBMC. (**e**) Graphical summary of proportion of $CD45^+$ cells of live cells in spleen and ES 18-34 days after PBMC transfer. n=3-6/experiment; cumulative data of 5 independent experiments. (**f**) Graphical summary of the proportion of $CD3^+$ cells of live $CD45^+$ cells (**g**) Representative flow cytometry analysis and graphical summary of $CD3^+$ percentages in ES and adjacent murine skin gated on live lymphocytes. n=3-6/experiment; cumulative data of 3 independent experiments. Significance determined by paired student's t test; mean $^+$/- SD. (**h**) Representative plots and graphical summary of TCR$\gamma\delta^+$ and $CD3^+$ cells of live $CD45^+$ in indicated tissues. (**i**) Representative flow cytometry plots of $CD4^+$ and $CD8^+$ of $CD3^+CD45^+$ live gated cells (**j**) Summary of CD4 and CD8 expressing cells in human PBMC and skin and spleen and ES, gated on live $CD3^+CD45^+$ lymphocytes. n=3-6/experiment; Combined data of 6 independent experiments.

Figure 2: Human CD4⁺ T cells maintain their functional cytokine profile in spleen and ES

(**a-c**) Single cell suspensions of blood and skin of healthy donors and spleen and ES of huPBMC-ES-NSG mice were stimulated *ex vivo* with PMA/ionomycin and intracellular cytokine production was analyzed by flow cytometry. Representative analysis of IL17, IL22, IL13, GM-CSF and IFNγ % of CD4⁺ cells as indicated and (**d**) CD25 and Foxp3 expression by gated CD4⁺CD3⁺CD45⁺ live leukocytes. (**e-j**) Graphical summary of the expression of the indicated markers by T cells from blood and skin of healthy donors and spleen and ES of huPBMC-ES-NSG mice by gated CD4⁺CD3⁺CD45⁺ live leukocytes. n=3-6/experiment; cumulative data of 2-5 independent experiments as indicated by the symbol fillings.

Figure 3: Human CD8⁺ T cells maintain their functional cytokine profile in spleen and ES

(**a-e**) Graphical summary of flow cytometry analysis of IL17, IL22, IL13, GM-CSF and IFNγ producing CD8⁺CD3⁺CD45⁺ gated live leukocytes from blood and skin of healthy donors and spleen and ES of huPBMC-ES-NSG mice as indicated upon *ex vivo* stimulation with PMA/Ionomycin and intracellular staining. n=3-6/ experiment; combined data of independent 1-4 experiments.

Figure 4: Skin and spleen infiltrating CD4⁺ T cells show skin-homing memory phenotype

Representative flow cytometry analysis of (**a**) CCR7 and CD45RA expression, and (**b**) CLA and CD45RA expression by gated CD4⁺CD3⁺CD45⁺ live leukocytes from blood and skin of healthy donors, spleen and ES of huPBMC-ES-NSG mice and graphical summary

of the proportions of indicated cells by gated $CD4^+CD3^+CD45^+$ live leukocytes. n=5-6/experiment; cumulative data of 2 independent experiments.

Figure 5: Cutaneous $CD4^+$ T Cells are activated by local APCs and remain responsive in allogeneic environment. (**a**) Schematic outline of the experiment. (**b**) Graphical summary of the proportion of $CD45^+$ cells among live cells in the lymphocyte gate in indicated organs of huPBMC-ES-NSG mice that received either LPS/moDC injections or HKCA/moDC injections into the ES. (**c**) Graphical analysis of the proportion of $Ki67^+$ proliferating cells and $CD25^+$ cells by gated $CD4^+CD3^+CD45^+$ live leukocytes from LPS/moDC or HKCA/moDC treated ES. n=2-7/experiment, cumulative data of 2-5 independent experiments. Statistical significance determined by 2-tailed unpaired student's t test; mean +/- SD. (**d**) Schematic: NSG mice bearing fully healed ES of one of two different skin donors (A and B) were adoptively transferred with either skin donor-matched PBMC or skin donor-mismatched PBMC. Intradermal injections of donor A derived LPS/moDC or HKCA/moDC were performed as depicted. Single cell suspensions of ES and spleen were analyzed by flow cytometry after *ex vivo* stimulation with PMA/Ionomycin and intracellular staining. (**e-h**) Graphical summary of the proportion of skin $CD4^+$ T cells expressing the indicated markers following intradermal encounter of LPS/moDC (LPS) or HKCA/moDC (HKCA). Red data points represent $CD4^+$ T cells isolated out of mismatched ES. Statistical significance determined by ANOVA and Tuckey's test for multiple comparison; mean +/-SD. (**i**) Graphical summary of the ratio between $CD4^+$ and $CD8^+$ T cells of isolated skin T cells gated by $CD3^+CD45^+$ live leukocytes.

Figure 6: Human skin and ES provide signals that support cutaneous T cell function

Cytokine and chemokine expression within tissues was determined by bead-based multicomponent analysis of ES from huPBMC-ES-NSG and 3 different healthy human skin donors. (**a-f**) Amount of the indicated chemokines or cytokines per mg skin. (**g**) huPBMC-NSG mice received intradermal injections of LPS/moDC or HKCA/moDC into a defined patch of murine skin on the back of the mouse or into ES of huPBMC-ES-NSG mice. Single cell suspensions of injected murine skin regions were analyzed by flow cytometry 7 days after last i.d. injection as indicated. **h)** Graphical summary of the proportion of $CD3^+$ T cells isolated from LPS/moDC (LPS) and HKCA/moDC (HKCA) injected murine skin and T cells isolated from the ES treated with HKCA/moDC (HKCA). Statistical significance determined by ANOVA and Tukey's test for multiple comparison; mean +/-SD

Supplemantary Figures

Supp.Fig.1: Human antigen-presenting cells do not engraft well in huPBMC-ES-NSG model. (**a**) Experimental procedure of the injection of $5x10^4$ free HKCA cells into the ES. Single cell suspensions of indicated organs were analyzed by flow cytometry. (**b**) Graphical summary of human $CD45^+$ cell proportions of live leukocytes in spleen and ES of mice that were left untreated (untrtd), injected with PBS or HKCA. (**c**) Representative flow cytometry analysis of $CD3^-HLA\text{-}DR^+$ cells in human PBMC, skin and spleen and ES of huPBMC-ES-NSG and (**d**) graphical summary gated on live $CD45^+$ cells.

Supp.Fig.2: Splenic T cell are not activated by HKCA presented in the ES. (**a-f**) Graphical summary of the expression of indicated markers by $CD4^+$ T cells of $CD3^+CD45^+$ live leukocytes isolated from the spleen of huPBMC-ES-NSG mice after intradermal injection of LPS/moDC (LPS) or HKCA/moDC (HKCA) upon *ex vivo* stimulation with PMA/ionomycin and intracellular cytokine staining. (**g**) Ratio of $CD4^+$ to $CD8^+$ cells in spleens of huPBMC-ES-NSG mice, gated on $CD3^+CD45^+$ live leukocytes.

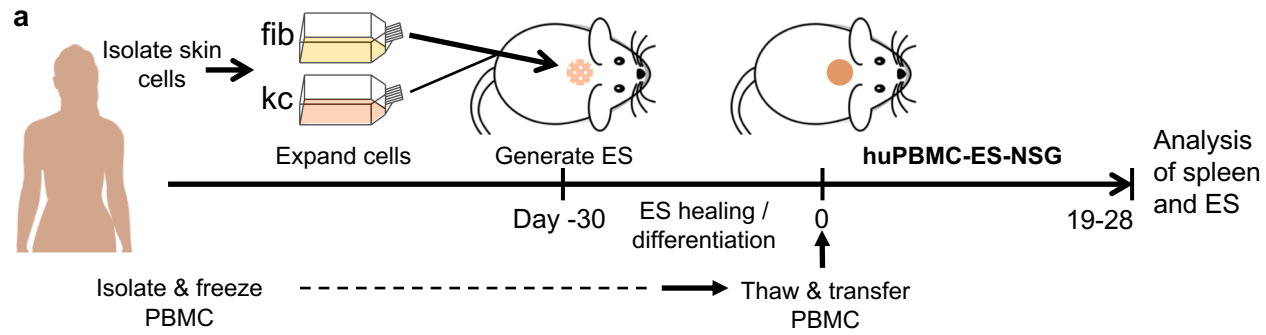

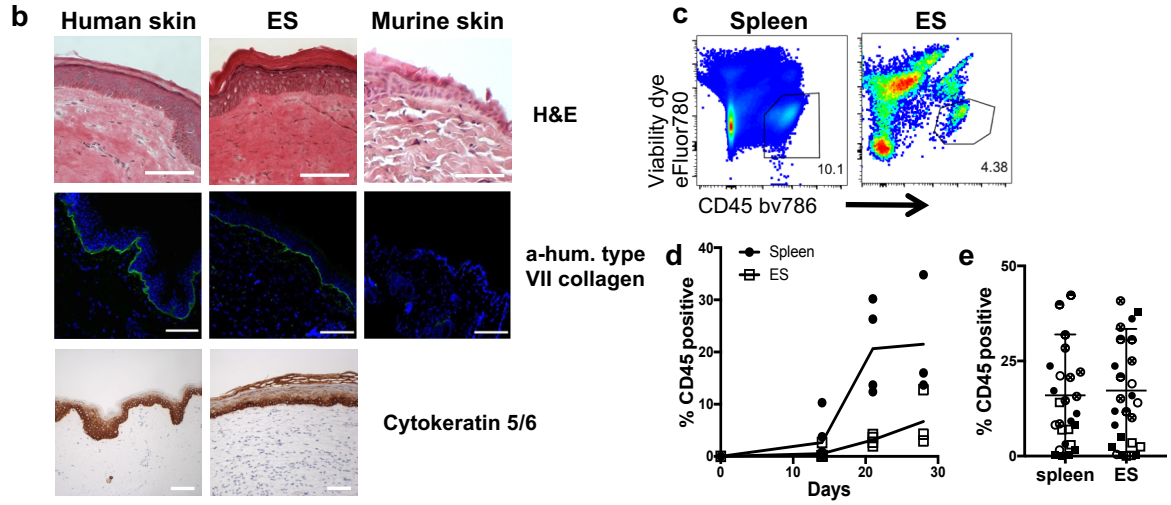

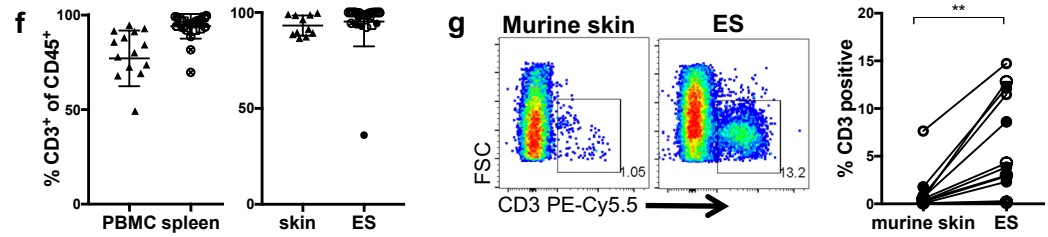

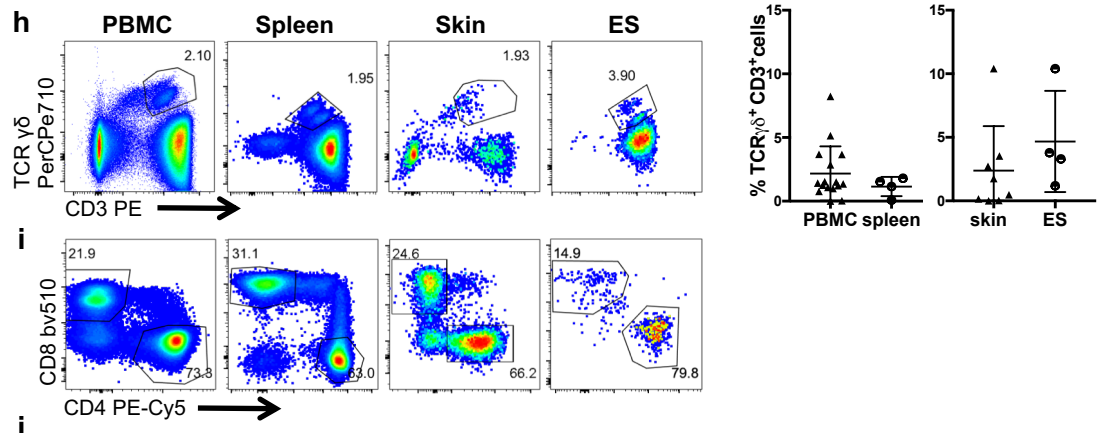

j

% positive	PBMC	Spleen	Skin	ES
CD4	65.54 +/- 9.687	58.62+/-18.44	64.49+/-11.98	69.48+/-20.66
CD8	22.3+/-8.114	30.74+/-16.32	26.67+/-11.39	19.16+/-12.72

Figure 1: Engineered skin resembles human skin and is preferentially infiltrated by human T cells upon adoptive PBMC transfer

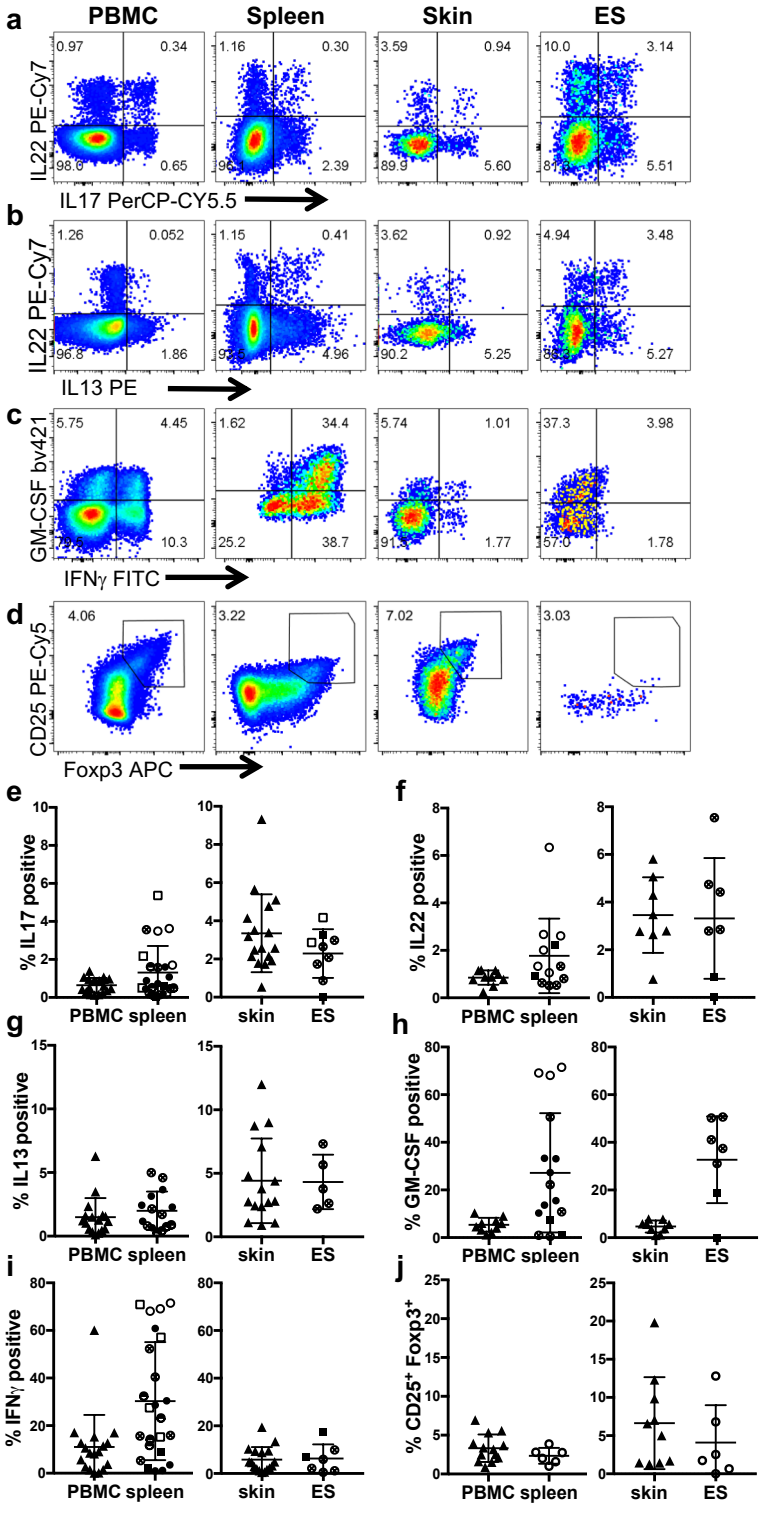

Figure 2: Human CD4⁺ T cells maintain their functional cytokine profile in spleen and ES

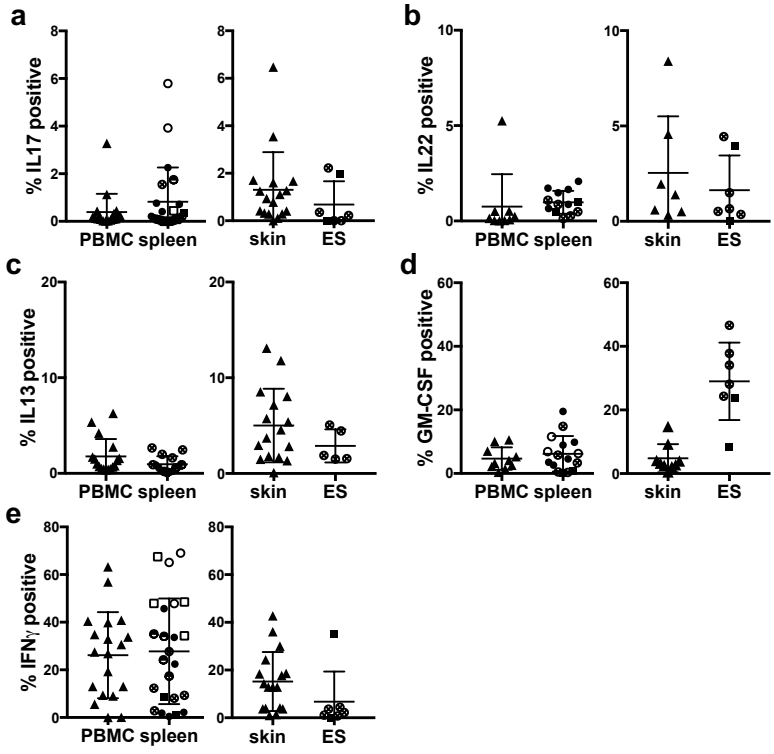

Figure 3: Human CD8^{+} T cells maintain their functional cytokine profile in spleen and ES

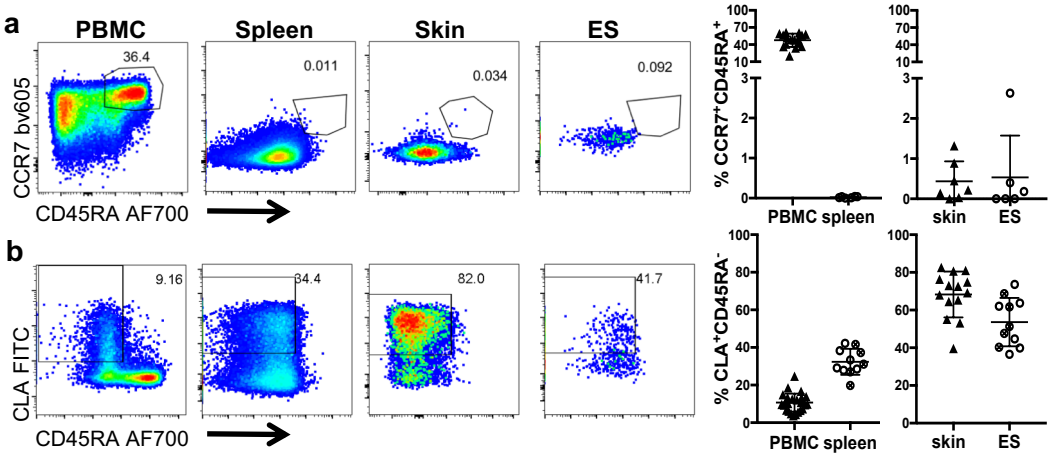

Figure 4: Skin and spleen infiltrating CD4⁺ T cells show skin-homing memory phenotype

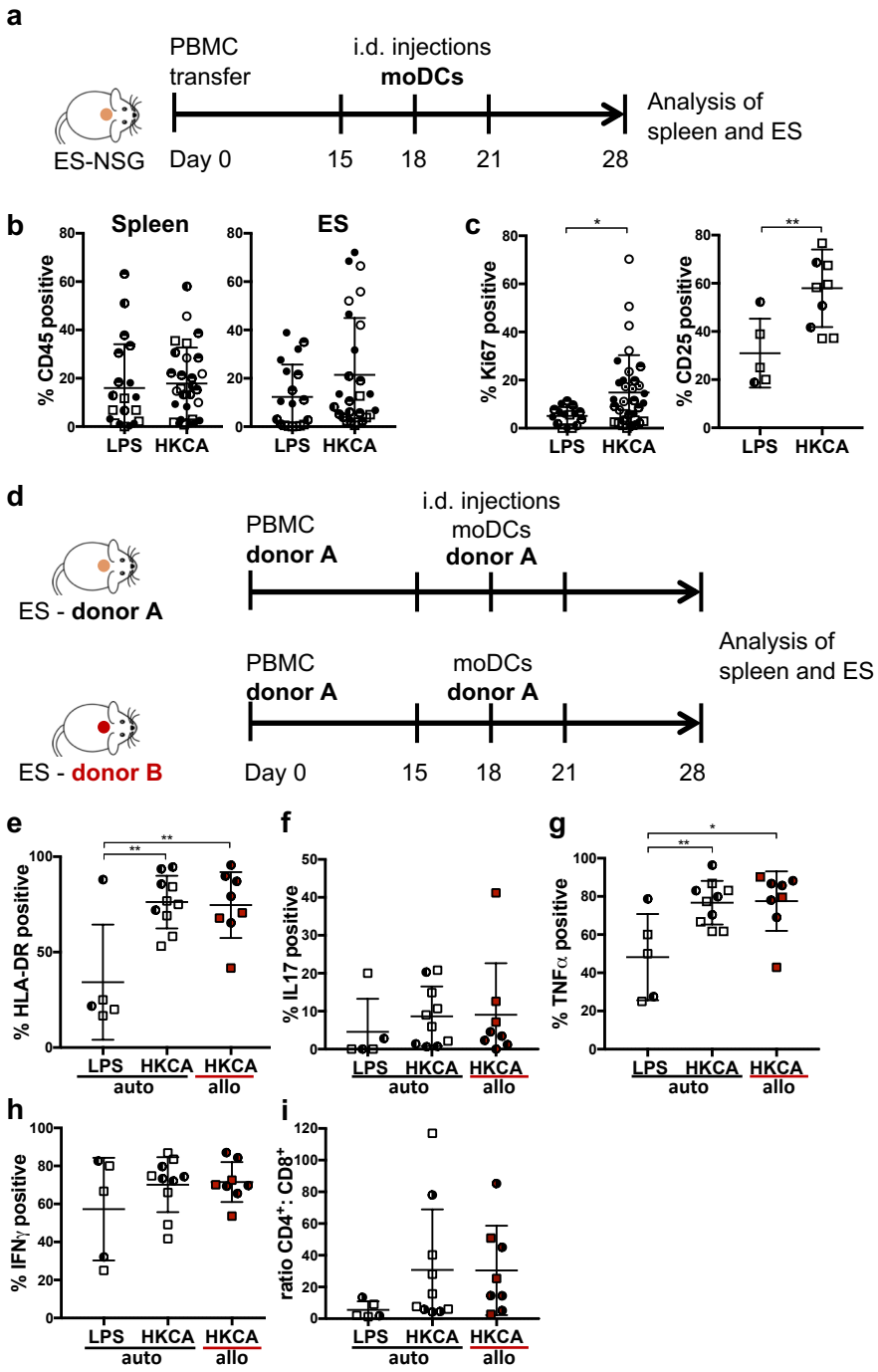

Figure 5: Cutaneous CD4⁺ T Cells are activated by local APCs and remain responsive in allogeneic environment.

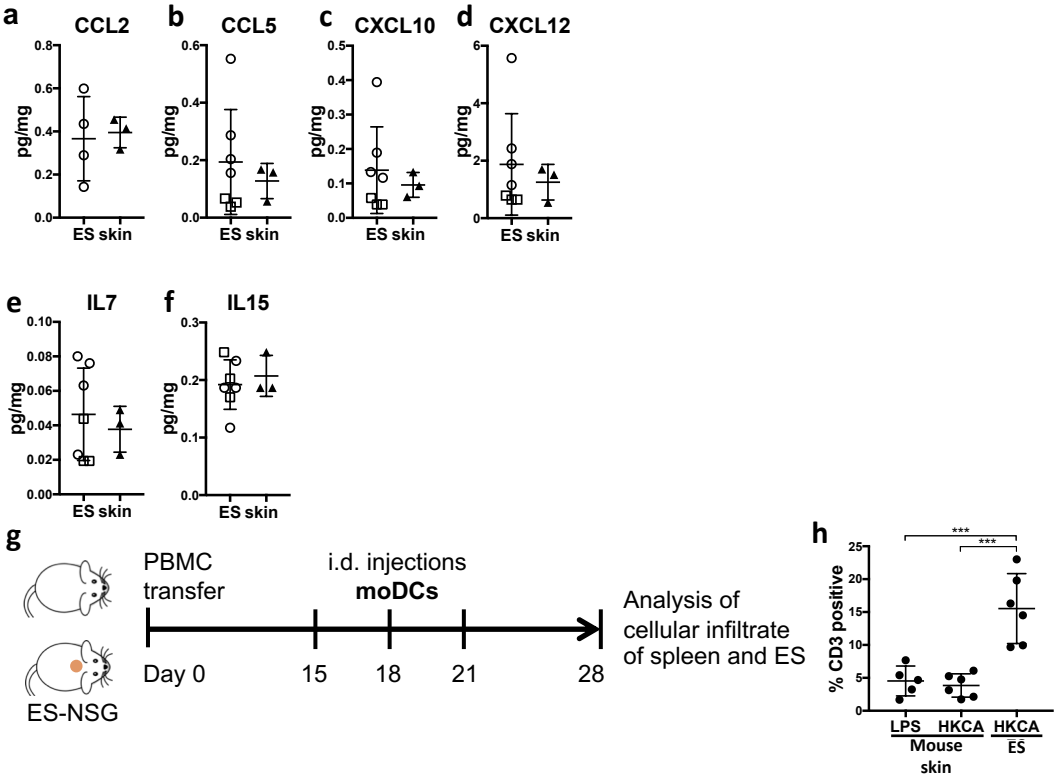

Figure 6: Human skin and ES provide signals that support cutaneous T cell function

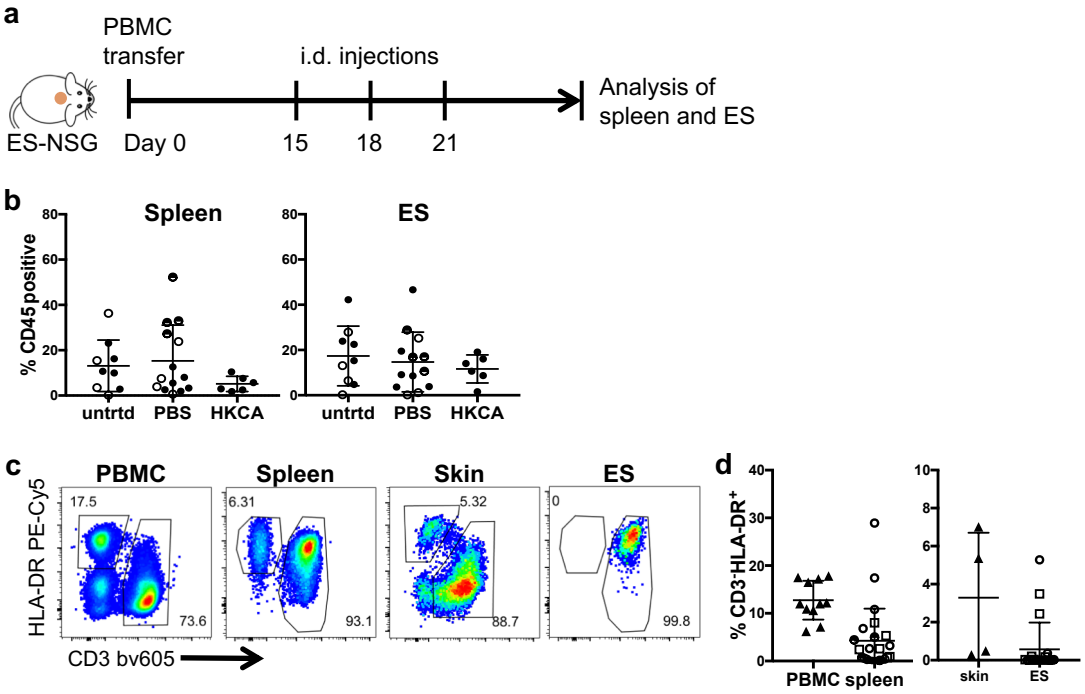

Supp.Fig.1: Human antigen-presenting cells do not engraft well in huPBMC-ES-NSG

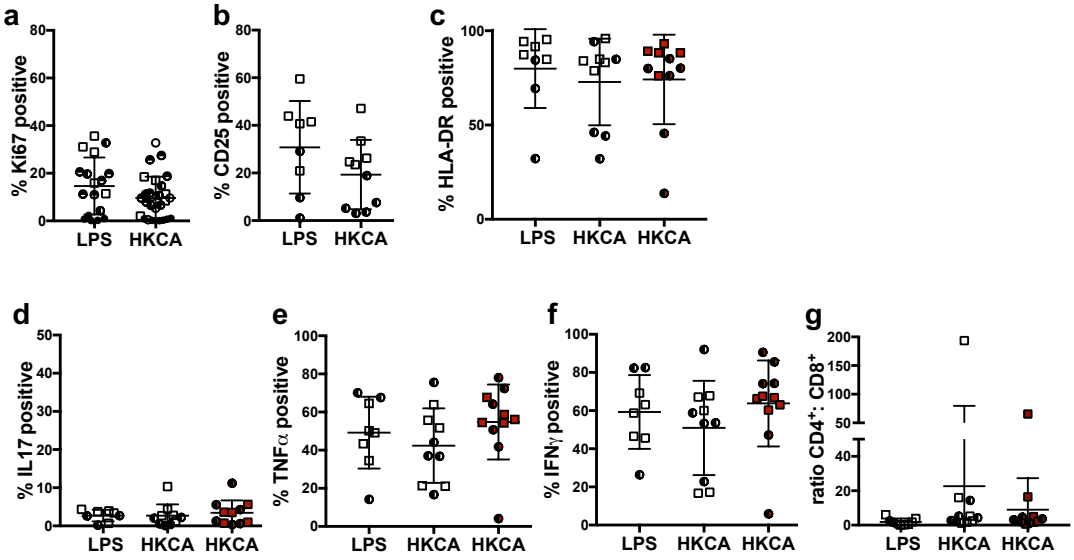

Supp.Fig.2: Splenic T cell are not activated by HKCA presented in the ES.

Table S1: Detailed list of antibodies and reagents

Tissue preparation

Reagent	Company	Catalog number
Collagenase Type 4	Worthington	LS004186
DNAse	Sigma-Aldrich	DN25
RPMI 1640	Gibco	31870074
human serum	Sigma-Aldrich	H5667/H4522
Penicillin/streptavidin	Sigma-Aldrich	P0781
L-Glutamine	Gibco	A2916801
NEAA	Gibco	11140035
Sodium-Pyruvat	Sigma-Aldrich	S8636
β-Mercaptoethanol	Gibco	31350-010
PBS	Gibco	14190169
Ficoll Paque Plus	GE-Healthcare	GE17-1440-02
Protease Inhibitor Cocktail	Sigma-Aldrich	P8340

Cellular activation

Reagent	Company	Catalog number
Brefeldin A	Sigma-Aldrich	B6542
Cytofix/Cytoperm kit	BD	RUO 554714
Foxp3 / Transcription Factor Staining Buffer Set	Invitrogen	00-5523-00
Ionomycin	Sigma-Aldrich	I06434
PMA	Sigma-Aldrich	P8139
Recombinant human IL2	Immunotools	11340023
Recombinant human IL4	Immunotools	11340047
Recombinant human GM-CSF	Immunotools	11343127
Purified NA/LE Mouse anti-human CD28 (CD28.2)	BD	555725
Functional Grade, CD3 monoclonal Antibody (OKT3)	eBioscience	16-0037-85
Cytokine/Chemokine/Growth Factor 45-Plex Human ProcartaPlex™	Invitrogen	EPX-450-12171-901

Skin cell culture and transplantation

Reagent	Company	Catalog number
Epilife	Gibco	MEPICF500
DMEM	Gibco	11960-044
MEM	Gibco	11380037
TrypLE express	Gibco	12604021
Primocin	invitrogen	ant-pm-1
X-VIVO 15	Lonza	881028

Tissue preparation from mice

Reagent	Company	Catalog number
BD Pharm Lyse	BD	555899
Collagenase from Clostridium histolyticum	Sigma-Aldrich	C9407
Hyaluronidase	Sigma-Aldrich	H3506

Histology

Reagent	Company	Catalog number
Cell Conditioning 1 (CC1)	Roche	950-124
Eosin Y aqueous solution	Sigma	HT110232
Hemalum solution acid acc. to Mayer	Carl Rorth	T865.1
Human Cytokeratin 5/6 (D5/16B4)	Roche	790-4554
ProLong™ Gold Antifade Mountant with DAPI	Invitrogen	P36931
TissueTek O.C.T. Compound	Sakura	TTEK
ultraView Universal DAB Detection kit	Roche	760-500

Antibodies

Reagent	Company	Catalog number
CLA FITC (HECA-452)	Biolegend	321306
CLA bv605 (HECA-452)	BD	563960
CD1a FITC (HI149)	BioLegend	300104
CD3 PerCP-Cy5.5 (OKT3)	eBioscience	45-0037-42
CD3 BV421 (UCHT1)	BioLegend	300434
CD3 bv605 (SK7)	BioLegend	344835
CD3 PE (HIT3a)	BD	561803
CD3 PE-Cy5.5 (UCHT1)	eBioscience	15-0038-42
CD4 PE-594 (RPA-T4)	BioLegend	300548
CD4 PE-Cy5 (RPA-T4)	BioLegend	300510
CD4 Alexa Fluor 700 (RPA-T4)	Biolegend	300526
CD4 bv500 (RPA-T4)	BD	560768
CD8 PE (OKT8)	eBioscience	12-0086-42
CD8 Pacific Orange (3B5)	eBioscience	MHCD0830
CD8 bv510 (RPA-T8)	BioLegend	301048
CD14 bv421 (M5E2)	BioLegend	301830
CD25 PE-Cy5	BioLegend	302608
CD25 PE-Cy7 (BC96)	eBioscience	302612
CD45 PerCP-Cy5.5 (HI30)	BD	564105
CD45 APC (HI30)	eBioscience	17-0459-42
CD45 BV785 (HI30)	BioLegend	304048
CD45RA PE-e610 (HI100)	eBioscience	61-0458-42
CD45RAPerCP-Cy5.5 (HI100)	BioLegend	304122
CD45RA Alexa Fluor 700 (HI100)	BioLegend	304120
CD86 PE (B7-2)	eBioscience	12-0869-41
CCR6 PE-Cy7 (G034E3)	BioLegend	353418
CCR7 bv605 (G043H7)	BioLegend	353224
Foxp3 APC (PCH101)	eBioscience	17-4776-42

Foxp3 eFluor450 (PCH101)	eBioscience	50-4776-41
GM-CSF bv421 (BVD2-21C11)	BD	562930
HLA-DR AF700 (L243)	BioLegend	307626
HLA-DR eFluor 780 (LN3)	eBioscience	47-9956-42
IFNg PE-Cy7 (B27)	BioLegend	506518
IFN-g BV605 (4S.B3)	BD	563731
IL-2 PE (MQ1-17H12)	eBioscience	12-7029-42
IL17A APC (BL168)	BioLegend	512334
IL-17A PerCP-Cy5.5 (eBio64DEC17)	eBioscience	45-7179-42
IL-13 PE (JES10-5A2)	BD	554571
IL-22 PE-Cy7 (22URTI)	eBioscience	25-7229-42
ki67 bv605 (ki67)	BioLegend	350521
ki-67 PE-Cy7 (SolA15)	eBioscience	25-5698-82
TNFa FITC (Mab11)	BioLegend	502915
TCRgd PerCP-eFluor710 (B1.1)	eBioscience	46-9959
Fixable Viability Dye eFluor™ 780	eBioscience	65-0865-14
Fixable Viability Dye eFluor™ 520	eBioscience	65-0867-14
eBioscience™ Fixable Viability Dye eFluor™ 506	eBioscience	65-0866-14
IF primary antibody: rabbit anti-human NC-1 domain of type VII collagen (LH7.2)	kindly provided by Dr. Alexander Nyström, University of Freiburg, Germany	
IF secondary antibody: goat anti-rabbit A488	ThermoFisher	A11008
mLy6G (Gr-1) InVivoMab RB6-8C5	BioXcell	BE0075
Cell Proliferation Dye eFluor™ 450	ThermoFisher	65-0842-85